

EROSION PROCESSES OF A NOVEL CONFIGURATION OF SEDIMENT REPLENISHMENT DURING AN ARTIFICIAL FLOOD

SEVERIN STÄHLY⁽¹⁾, MÁRIO J. FRANCA⁽²⁾, CHRISTOPHER T. ROBINSON⁽³⁾ & ANTON J. SCHLEISS⁽⁴⁾

^(1,4) Laboratoire de Constructions Hydrauliques (LCH), École Polytechnique Fédérale de Lausanne (EPFL), Lausanne, Switzerland
e-mail : sev.staehly@gmail.com, anton.schleiss@epfl.ch

⁽²⁾ Water Science and Engineering Department, Delft Institute for Water Education (UN-IHE), Delft, The Netherlands
e-mail : m.franca@un-ihe.org

⁽²⁾ Department of Hydraulic Engineering, Delft University of Technology, Delft, The Netherlands
e-mail : m.j.franca@tudelft.nl

⁽³⁾ Department of Aquatic Ecology, Swiss Federal Institute of Aquatic Science and Technology (EAWAG), Dübendorf, Switzerland
e-mail : christopher.robinson@eawag.ch

ABSTRACT

Floodplains downstream of dams with constant residual flow discharge often lack sediment supply and periodic inundation due to the absence of flood events. At the Sarine floodplain in Fribourg, western Switzerland, an artificial flood was released from Rossens Dam in 2016. This flood was combined with a novel configuration of sediment replenishment. The replenishment design was tested previously in laboratory experiments but not in the field. To investigate the erosion processes of the replenishment design, 489 stones with an average *b*-axis of 5.7 or 11.3 cm were equipped with RFID PIT tags and mixed in the replenished sediment. Downstream of the replenishment area, a pass-over loop fix-antenna was installed in the river to record passing PIT tags. With a mobile antenna, PIT tags were relocated after the flood. Peak discharge of the flood corresponded to a flood with a return period of two years; bankful discharge was observed during the flood peak. With the information of the fix-antenna, an average transport velocity for both PIT-tagged sediment sizes was calculated. Applying this measured transport velocity on all transported and post-flood detected stones allowed calculation of the erosion time for each stone and sediment deposit. The results show that the rising limb of the hydrograph is significantly more effective in mobilizing replenishment material than the decreasing limb. These findings are in line with observations made in the laboratory experiments.

Keywords: *RFID PIT tags, hydropower, artificial flood, sediment transport velocity, fixed antenna*

1 INTRODUCTION

Flow and sediment regimes can induce a large variety of habitats to rivers (Allan & Castillo, 2007; Wohl et al., 2015). Hydro-morphological conditions are an essential factor for in-stream life. Species have preferred ecohydraulic conditions, including flow depths, velocities and shear stresses near the streambed (Heggenes, 1996; Statzner et al., 1988). The natural flow regime as well as the temporal and spatial ecohydraulic diversity are often altered by the construction of dams (Moyle & Mount, 2007). Dams trap sediment in the upstream reservoir and interrupt the sediment continuum, what can cause severe deficits in the downstream river segment (Kondolf, 1997; Petts & Gurnell, 2005).

To counteract these deficits, sediment replenishment combined with the release of artificial flood events have been widely studied and applied (Arnaud et al., 2017; Battisacco et al., 2016; Gaeuman, 2012; Gaeuman et al., 2017; Heckmann et al., 2017; Robinson, 2012; Robinson et al., 2018; Staentzel et al., 2018; Stähly et al., 2018). The sediment is placed in the river with different techniques and with an artificial flood pulse distributed in the river (Ock et al., 2013).

In the study presented here, the transport behavior of a sediment replenishment was investigated with Radio Frequency Identification Passive Integrated Transponder (RFID PIT) tags and a fix-installed pass-over antenna in the Sarine River in 2016. This was tested combined with a novel configuration of a multi-deposit sediment replenishment methodology, consisting of four alternating bars, two along each river bank (Figure 1). This configuration was tested the first time in the field after obtaining promising results from an extensive laboratory study (Battisacco, 2016). The interest was to evaluate how far the replenished sediment was transported and which period of the hydrograph was most efficient for sediment entrainment.



Figure 1. Deposits I to IV in the experiments of Battisacco et al. (2016). Deposit I was located the most upstream, deposit IV the most downstream.

2 SITE DESCRIPTION

The Sarine is located in western Switzerland and drains a catchment of 1900 km². It is 126 km long before joining the Aare, a tributary of the Rhine, ending in the Northern Sea. The Rossens Dam, constructed in 1948 (dam foot on 608 m a.s.l.), is one of the six reservoirs along the main stem of the river. It creates the 200 Mio m³ large reservoir Lac de la Gruyère, releasing a 2.5–3.5 m³/s residual flow to the about 13 km long river segment between the dam and the power house in Hauterive (see Figure 2). The 13 km long reservoir retains all incoming sediment and makes spilling rare (Figure 3). This river segment has a wetted width of 20-35 m and a bed slope of 0.3 %.

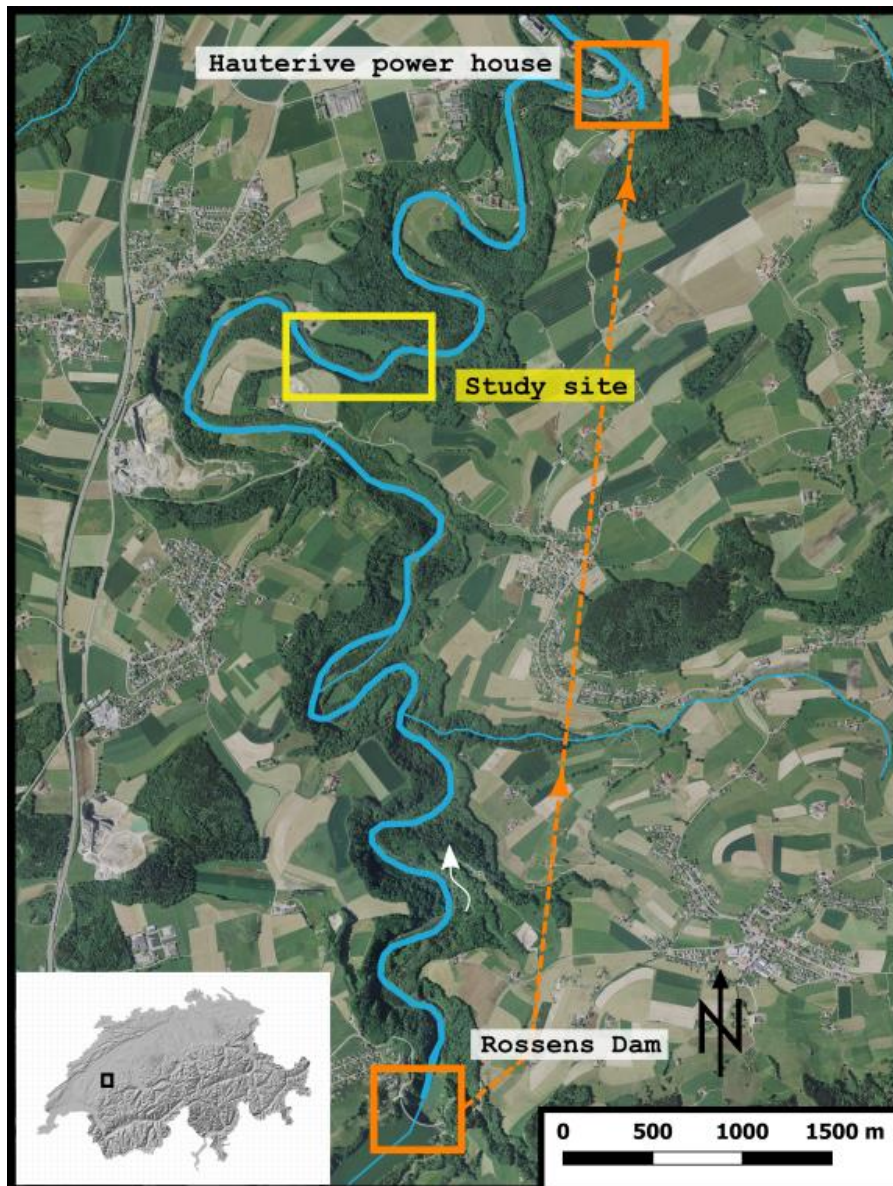


Figure 2. Overview of the residual flow river segment of the Sarine between the Rossens Dam and the power house in Hauterive. The four deposits were added to the study site analog to Figure 1, consisting of four deposits, deposit I at the upstream and deposit IV at the downstream end of the measure.

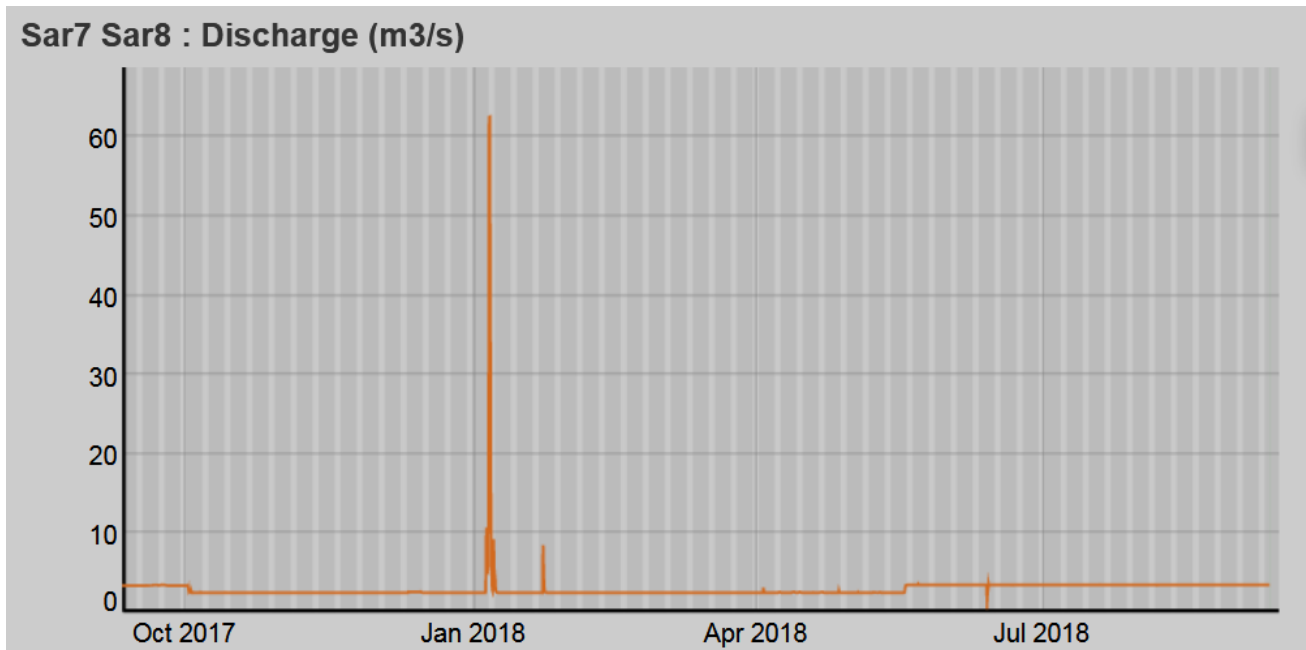


Figure 3. Discharge over a year downstream of Rossens Dam. The highest released discharge of about 60 m³/s is clearly below the discharge with a return period of one year ($HQ_1 \approx 110$ m³/s). Figure obtained from www.swissrivers.ch, webpage consulted on 12 September 2018.

3 METHODOLOGY

3.1 Multi-deposit replenishment configuration

The replenishment was added in four deposits of sediment and placed in the river at the coordinates 46°45'29.21"N / 7°06'11.47"E (see Figure 1 and 2). From a river management and sustainability point of view it would be more reasonable to replenish the Sarine River with sediment directly downstream of the Rossens Dam. The configuration was an adaptation to field conditions of the sediment replenishment successfully tested previously in flume experiments (Battisacco, 2016). In total the river was replenished with 1000 m³ sediment, divided into four deposits of about 250 m³ each (Figure 3). As comparison, before the dam construction 4'000 to 8'000 m³ sediment was transported in this river segment every year. Figure 4 shows an example of one sediment deposit. The deposit width W was about 8 m and the length L 22 m. The height of the deposits varied spatially depending on river bed elevation and was about 1.5 m in average. The replenished sediment was excavated from the adjacent alluvial forest on the right side of the river. Since the excavation came from the floodplain, no washing or sorting could be applied. The grain size distribution (GSD) corresponded to the material found in the river bed. While the sediment was put in place, lots of fine sediment was released to the river. Where the sediment was excavated, ponds with still water were created, serving as new habitats for amphibians.



Figure 4. Deposit I and III in the Sarine looking upstream. Image courtesy: Elena Battisacco

3.2 Sediment tracking system

The excavated material was composed of characteristic grain sizes $d_m = 57$ mm and $d_{90} = 113$ mm. The grain size distribution was determined analyzing 21 samples of Fehr line-sampling (Fehr, 1987) and photo sieving using BASEGRAIN (Stähly et al., 2017). A total of 489 stones, divided in d_m and d_{90} , were collected in the field, drilled and the hole filled with a Radio Frequency Identification Passive Integrated Transponder tag (RFID PIT tag) of 32 mm and 23 mm length and sealed with silicon (Arnaud et al., 2015; Brenna et al., 2019; Cassel et al., 2017). With the software S2_Util (Texas Instruments TIRIS, Version 1.20), tags were programmed with a unique identification number. After measuring the three axes and the weight of the tagged stones, they were distributed equally in three layers (top, middle and bottom) in the four deposits.

About 100 m downstream of deposit IV, a pass-over loop fix-antenna was mounted across the river, perpendicular to the main flow direction (Schneider et al., 2010). The antenna consisted of a single loop multiple-strand cable with a diameter of 16 mm², protected by a rubber hose (Figure 5). The hose was fixed with cable straps close to the river bed at 1 m long armoring irons that were vertically installed into the river bed every meter. Prior to its installation, the antenna shape was optimized to a length corresponding to the local river width of about 25 m. The optimal antenna surface of 25 m x 0.3 m resulted in a detection distance of up to 1.5 m under dry conditions. Installed in the river, the detection distance below water did not exceed 0.3 m.

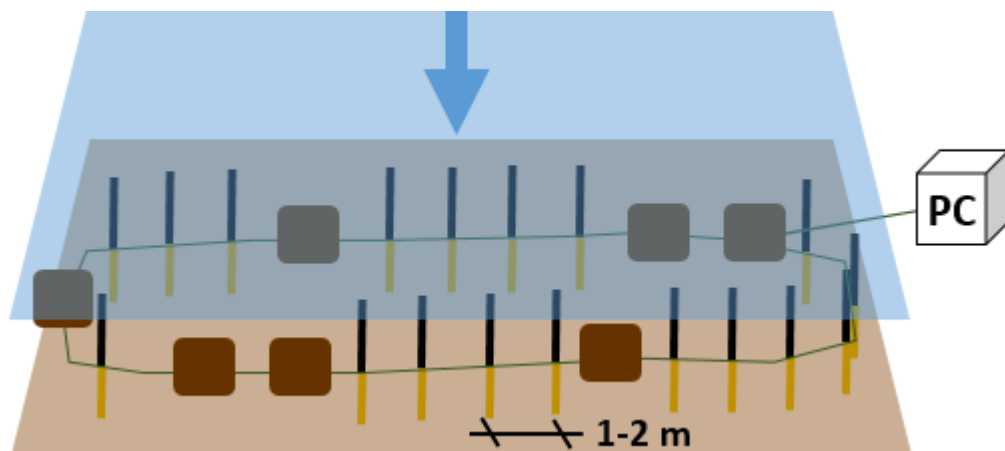


Figure 5. Drawing of the pass-over loop fix antenna in the Sarine. The brown squares are large stones of the river bed, the vertical lines are iron bars. The cable was protected with a garden hose which was fixed with cable straps on the irons. The irons were one m long and rammed in the river with a distance of one to two meters.

In addition to the fixed antenna, a mobile antenna was used for RFID PIT tag detection after the flood. The mobile antenna consisted of a 1.5 m long pole and 0.7 m diameter ring attached at the end, both made of plastic (Figure 6). Inside the ring, a double loop of 4 mm² multiple-strand cable formed the antenna. The electro-magnetic components are carried in a back pack. When detecting a PIT tag, the electromagnetic components beeped and the tag ID appeared on a little screen. Both antenna systems, the fixed and the mobile antenna, worked with a 12 V 7.0 Ah battery. The electromagnetic components, such as the PIT tags, Tuning Board, HDX Reader and Control board are products from OREGON RFID, Portland, USA. The PIT tags work at a low frequency of 134.2 kHz, allowing detection in submerged conditions.



Figure 6. Searching for tags after the artificial flood event with the mobile antenna to determine the final position x_d of the tagged stones.

With the help of the self-made mobile RFID antenna, the location of tagged stones could be detected after the flood event and their locations were recorded with a differential Global Navigation Satellite System (GNSS, model TOPCON HiPer Pro) with an accuracy of a few centimeters. The location of origin x_0 and deposition x_d for tagged stones could therefore be captured with a precision of about 1 m due to the antenna-size. The location of the fix-antenna x_a was known. In addition, the zone of erosion was defined, covering the influence area of the deposits where flow varies highly. It reaches from the upstream end of deposit I until one river width downstream of deposit IV x_e . The definition of this spatial division is given in Figure 7.

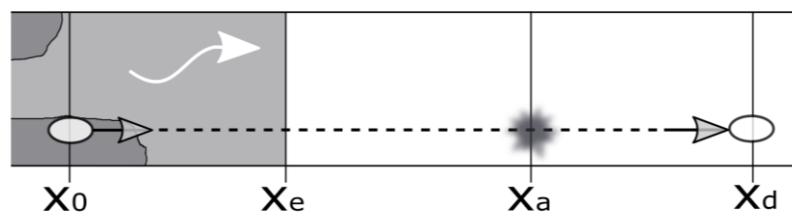


Figure 7. Concept and sketch of the longitudinal scales. The erosion zone is shaded, deposit III and IV dark gray. x_0 = original position where a tagged stone was put in the sediment deposit; x_e = downstream end of the erosion zone; x_a = location of the pass-over loop fix-antenna; x_d = final position where a tagged stone was found after the flood event.

Knowing the location of deposition of a tagged stone x_d , the time it ceased moving t_d , the time it passed the antenna t_a and the location of the antenna x_a , an average transport velocity v_d for each stone that passed the fix-antenna can be estimated for the distance between the fix-antenna and the location of final settling (Equation 1). This measured average transport velocity, referred to as virtual velocity v_d , is the average of a series of bouncing and stopping processes within the interval of x_a and x_d in the allocated time period (Hassan et al., 1991). On the other hand, the velocity upstream the antenna can be calculated based on the time and location at the antenna (t_a , x_a) with its departing location (x_0) and earliest possible moment for erosion (t_0). The erosion time t_e indicates the time a tagged stone is transported out of the erosion zone and can be obtained by Equation 2 (see Figure 8).

This allows then the determination of the erosion-effective periods during the flood event as well as the corresponding sedigraph representing the time-series of the erosion of the tagged stones. Based on the

sedigraph and on the released volume a parameter called erosion efficiency is introduced (*eff*, see Equation 3), which corresponds to the ratio between the percentage of eroded tags in a certain time period i (Δt_i) and the percentage of released water during the same time period.

$$v_d = \frac{x_d - x_a}{t_d - t_a} \quad [1]$$

$$t_e = t_d - \frac{x_d - x_e}{v_d} \quad [2]$$

$$eff = \frac{\text{Eroded tagged stones (during } \Delta t_i \text{)} [\%]}{\text{Released water volume (during } \Delta t_i \text{)} [\%]} \quad [3]$$

where,

- eff* : Erosion efficiency
- Δt_i : i -th time interval
- t_a : Time of the stone passing the antenna
- t_d : Time of deposition of the stone
- t_e : Time the tagged stone leaves the erosion zone
- v_d : Average stone transport velocity
- x_a : Location of antenna
- x_d : Location of settling
- x_e : Downstream end of the erosion zone

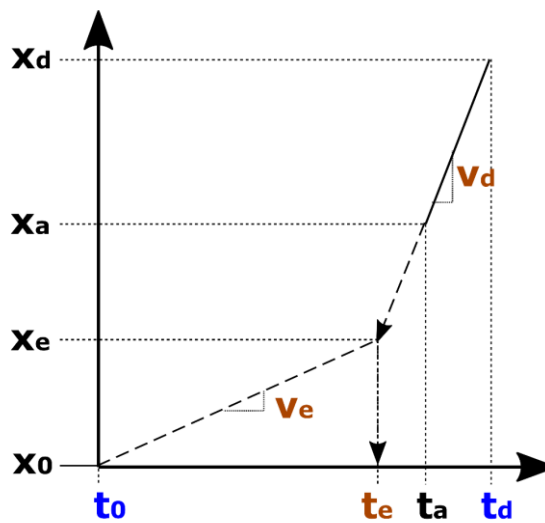


Figure 8. Concept of the estimation of the average sediment transport velocity or virtual velocity v_d and erosion velocity v_e ; x_0 = original position where a tagged stone was put in the sediment deposit; x_e = downstream end of the erosion zone; x_a = location of the pass-over loop fixed-antenna; x_d = final position where a tagged stone was found after the flood event. t_0 = time of erosion; t_e = time of leaving the erosion zone; t_a = time of passing the pass-over loop fixed-antenna; t_d = time the stone stopped moving. **Blue** = estimated values, **brown** = calculated values.

3.3 Critical discharges to determine t_0 and t_d

The critical discharge for the d_m and d_{90} on each deposit was determined using a numerical 2D-flow-model in BASEMENT v2.6, which is a freeware simulation tool for hydro- and morphodynamic modeling (for more information, see www.basement.ethz.ch). The mesh was constructed in QGIS using the plugin BASEmesh flood. The used critical discharges are the given in Table 1.

Table 1. Critical discharges taken for the estimation of virtual velocity and erosion time. Values used for the calculation were chosen based on the numerical model results and field observations. As a deposition criterion, the smallest discharge taken for the incipient erosion was used for each deposit.

DEPOSIT	INCIPIENT MOTION Q		DEPOSITION Q	
	D_M [M ³ /s]	D_{90} [M ³ /s]	D_M [M ³ /s]	D_{90} [M ³ /s]
I	34	106	84	29
II	72	137	84	29
III	29	84	84	29
IV	53	122	84	29

4 RESULTS

The artificial flood had a peak discharge corresponding to a return period of two years. The four sediment deposits were eroded partially (Stähly et al., 2019). In total, 84 tagged stones were detected with the mobile antenna downstream of the erosion zone. Six PIT tag equipped stones were registered at the pass-over loop fixed antenna. From these six stones, only two could be used to calculate the erosion time t_e , one d_m and one d_{90} (Equations 1 and 2).

For the analysis of the virtual velocities, values for critical discharge were taken based on the numerical model results, allowing the determination of t_0 and t_d (Table 1). The virtual velocity v_d resulted in 19 cm/min (equal to $3.1 \cdot 10^{-3}$ m/s) for the d_m and 28 cm/min (equal to $4.6 \cdot 10^{-3}$ m/s) for the d_{90} . These two values were then assigned to all 84 tagged stones that were transported further than the lower boundary of the erosion zone and detected with the mobile antenna after the flood event. This allowed the calculation of the erosion time t_e for each tag (Figure 9).

The most effective erosion occurred after the discharge reached 175 m³/s. Once the discharge passed its maximum and decreased, the erosion diminished quickly and equaled zero, once the discharge was below 126 m³/s. The sedigraph in Figure 9 indicates high erosion mainly during increasing discharge. Four periods of steep increase in discharge until 12 h, intermediated by constant discharge periods, are observed. About 40 % of the stones were transported during these periods of steep increase of the discharge, which represented only 20 % of the water released. This is associated with an erosion efficiency $eeff$ of 2.16 for the steep increase of the discharge.

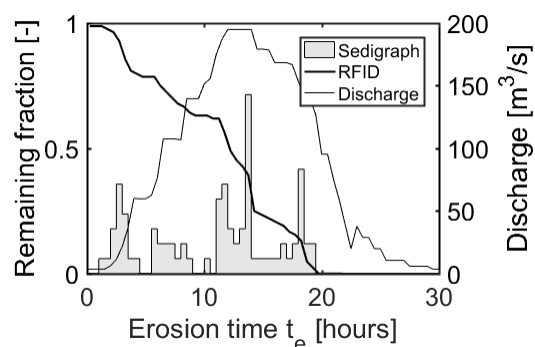


Figure 9. The erosion time represents the time that the 84 stones took to leave the erosion zone. The survivor function (Davison & Hinkley, 1997) indicates the proportion of stones remaining in the erosion zone (84 stones = 100 %). To cluster the data, a censored analysis was done assembling all PIT tag-equipped stones leaving the zone within a change in discharge of 15 m³/s or higher. The sedigraph (shaded) is for illustrative purposes and does not correspond to a y-axis, highest point at 0.14.

5 CONCLUSIONS

The herein presented methodology with the case study Sarine River serves as an example to calculate the average sediment transport velocity based on in-situ measurements. The fixed installed antenna did not work properly during the whole event hence a more rigid construction needs to be applied in field experiments. The strong forces and high shear stresses acting at the bottom of the Sarine during the flood event changed the shape of the antenna permanently and with it the electromagnetic field. Despite all the vertically installed metal rods staying in place, the hose was detached from some rods and the cable straps broke, resulting in a high

flexibility of the antenna shape. A relatively flexible system has the advantage that it tolerates a certain amount of impact by rolling, jumping and sliding rocks, whereas a complete rigid structure may completely break after impact and no data would be collected. Additionally, the antenna is more tolerant to bed erosion.

The erosion efficiency on the other hand can serve as an important tool for dam operators to optimize flood pulses. It is clear that the variation in shape and weight of tagged stones is not taken into account in the presented results, however the conclusion that the main erosion happens during increasing discharge covers with other studies (Robinson, 2012).

ACKNOWLEDGEMENTS

This research project was part of the National Research Programme "Energy Turnaround" (NRP 70, www.nrp70.ch) of the Swiss National Science Foundation (SNSF, Project No. 153972) and the Swiss Federal Office of Energy (SFOE, Project No. 501673-01). Anthony Maître contributed in the framework of his master thesis to the field data collection. Jonas Durand-Gasselín, Elena Battisacco and Diego Tonolla helped during the field campaigns in the Sarine River.

REFERENCES

- Allan, J.D., & Castillo, M.M. (2007). *Stream ecology: Structure and function of running waters: Second edition. Stream Ecology: Structure and Function of Running Waters: Second Edition*. Dordrecht, The Netherlands: Springer. 436pp.
- Arnaud, F., Piégay, H., Béal, D., Collery, P., Vaudor, L., & Rollet, A.J. (2017). Monitoring gravel augmentation in a large regulated river and implications for process-based restoration. *Earth Surface Processes and Landforms*, 42(13), 2147–2166.
- Arnaud, F., Piégay, H., Vaudor, L., Bultingaire, L., & Fantino, G. (2015). Technical specifications of low-frequency radio identification bedload tracking from field experiments: Differences in antennas, tags and operators. *Geomorphology*, 238, 37–46.
- Battisacco, E. (2016). *Replenishment of sediment downstream of dams: erosion and transport processes*. EPFL Ph.D Thesis No. 7293 and Communication 67 of Laboratory of Hydraulic Constructions (Ed. A. Schleiss), Ecole polytechnique fédérale de Lausanne (EPFL). Lausanne.
- Battisacco, E., Franca, M.J., & Schleiss, A.J. (2016). Sediment replenishment: Influence of the geometrical configuration on the morphological evolution of channel-bed. *Water Resources Research*, 52(11), 8879–8894.
- Brenna, A., Surian, N., & Mao, L. (2019). Virtual Velocity Approach for Estimating Bed Material Transport in Gravel- Bed Rivers: Key Factors and Significance. *Water Resources Research*, 55.
- Bunte, K., & Abt, S.R. (2001). *Sampling Surface and Subsurface Particle-Size Distributions in Wadable Gravel- and Cobble-Bed Streams for Analyses in Sediment Transport, Hydraulics, and Streambed Monitoring*.
- Cassel, M., Piégay, H., & Lavé, J. (2017). Effects of transport and insertion of radio frequency identification (RFID) transponders on resistance and shape of natural and synthetic pebbles: applications for riverine and coastal bedload tracking. *Earth Surface Processes and Landforms*, 42(3), 399–413.
- Davison, A.C., & Hinkley, D.V. (1997). *Bootstrap Methods and their Application*. New York, USA: Cambridge University Press.
- Fehr, R. (1987). *Geschiebeanalysen in Gebirgsflüssen. Mitteilungen der Versuchsanstalt für Wasserbau, Hydrologie und Glaziologie*. Mitteilungen der Versuchsanstalt für Wasserbau, Hydrologie und Glaziologie Nr. 92 (Ed. D. Vischer). Swiss Federal Institute of Technology (ETH) Zurich, Switzerland.
- Gaeuman, D. (2012). Mitigating Downstream Effects of Dams. In M. Church, P. M. Biron, & A. G. Roy (Eds.), *Gravel-Bed Rivers: Processes, Tools, Environments* (pp. 182–189). John Wiley & Sons Ltd.
- Gaeuman, D., Stewart, R., Schmandt, B., & Pryor, C. (2017). Geomorphic response to gravel augmentation and high-flow dam release in the Trinity River, California. *Earth Surface Processes and Landforms*, 42(15), 2523–2540.
- Hassan, M.A., Church, M., & Schick, A.P. (1991). Distance of movement of coarse particles in gravel bed streams. *Water Resources Research*, 27(4), 503–511.
- Heckmann, T., Haas, F., Abel, J., Rimböck, A., & Becht, M. (2017). Feeding the hungry river: Fluvial morphodynamics and the entrainment of artificially inserted sediment at the dammed river Isar, Eastern Alps, Germany. *Geomorphology*, 291, 128–142.
- Heggenes, J. (1996). Habitat selection by brown trout (*Salmo trutta*) and young Atlantic salmon (*S-salar*) in streams: Static and dynamic hydraulic modelling. *Regulated Rivers-Research & Management*, 12(July 1994), 155–169.
- Kondolf, G.M. (1997). HungryWater: Effects of Dams and Gravel Mining on River Channels. *Environmental Management*, 21(4), 533–551.
- Moyle, P.B., & Mount, J.F. (2007). Homogenous rivers, homogenous faunas. *Proceedings of the National Academy of Sciences*, 104(14), 5711–5712.

- Ock, G., Sumi, T., & Takemon, Y. (2013). Sediment replenishment to downstream reaches below dams: implementation perspectives. *Hydrological Research Letters*, 7(3), 54–59.
- Petts, G.E., & Gurnell, A.M. (2005). Dams and geomorphology: Research progress and future directions. *Geomorphology*, 71(1–2), 27–47.
- Robinson, C.T. (2012). Long-term changes in community assembly, resistance, and resilience following experimental floods. *Ecological Applications : A Publication of the Ecological Society of America*, 22(7), 1949–1961.
- Robinson, C. T., Siebers, A. R., & Ortlepp, J. (2018). Long-term ecological responses of the River Spöl to experimental floods. *Freshwater Science*, 433–447.
- Schneider, J., Hegglin, R., Meier, S., Turowski, J. M., Nitsche, M., & Rickenmann, D. (2010). Studying sediment transport in mountain rivers by mobile and stationary RFID antennas. *River Flow*, 1723–1730.
- Staentzel, C., Arnaud, F., Combroux, I., Schmitt, L., Trémolières, M., Grac, C., ... Beisel, J. N. (2018). How do instream flow increase and gravel augmentation impact biological communities in large rivers: A case study on the Upper Rhine River. *River Research and Applications*, 34(2), 153–164.
- Stähly, S., Franca, M. J., Robinson, C. T., & Schleiss, A. J. (2019). Sediment replenishment combined with an artificial flood improves river habitats downstream of a dam. *Scientific Reports*, 5176(9).
- Stähly, S., Friedrich, H., & Detert, M. (2017). Size Ratio of Fluvial Grains' Intermediate Axes Assessed by Image Processing and Square-Hole Sieving. *Journal of Hydraulic Engineering*, 143(6), 6017005.
- Stähly, S., Maître, A., Franca, M.J., Robinson, C.T., & Schleiss, A.J. (2018). Experiments with sediment replenishment in a residual flow reach: Comparison of field data with laboratory experiments. In A. Paquier & N. Rivière (Eds.), *9th International Conference on Fluvial Hydraulics River Flow 2018*, p. 2022.
- Statzner, B., Gore, J.A., & Resh, V.H. (1988). Hydraulic Stream Ecology: Observed Patterns and Potential Applications. *Journal of the North American Benthological Society*, 7(4), 307–360.
- Wohl, E., Bledsoe, B.P., Jacobson, R.B., Poff, N.L., Rathburn, S.L., Walters, D.M., & Wilcox, A.C. (2015). The natural sediment regime in rivers: Broadening the foundation for ecosystem management. *BioScience* 65(4), 358-371.
- Zingg, T. (1935). Beitrag zur Schotteranalyse. *Schweizerische Mineralogisch-Petrographische Mitteilungen*, 15, 39–140.